Current Biology, Volume *22*
Supplemental Information

Octopamine Neurons Mediate Flight-Induced Modulation of Visual Processing in *Drosophila*

Marie P. Suver, Akira Mamiya, and Michael H. Dickinson

Supplemental Inventory

Supplemental Figures

Figure S1: Control for length/design of octopamine pharmacology experiment outlined in Figure 2. This figure supports that the effect we attribute to octopamine pharmacology in Figure 2 is not due to the sequence or length of the experiment.

Figure S2: Shows effect of flight during octopamine application, related to Figure 2. Figure 2 outlines the effect of octopamine pharmacology, but the additional effect of flight shown here supports the notion that the baseline shift is not mediated by octopamine neurons, as described in the Discussion.

Figure S3: Shows effect of flight during activation of octopamine neurons, related to Figure 4 and Figure S2. Figure 4 outlines the effect of octopamine neuron activation, and is relevant to our discussion of the origin of the baseline shift.

Supplemental Experimental Procedures

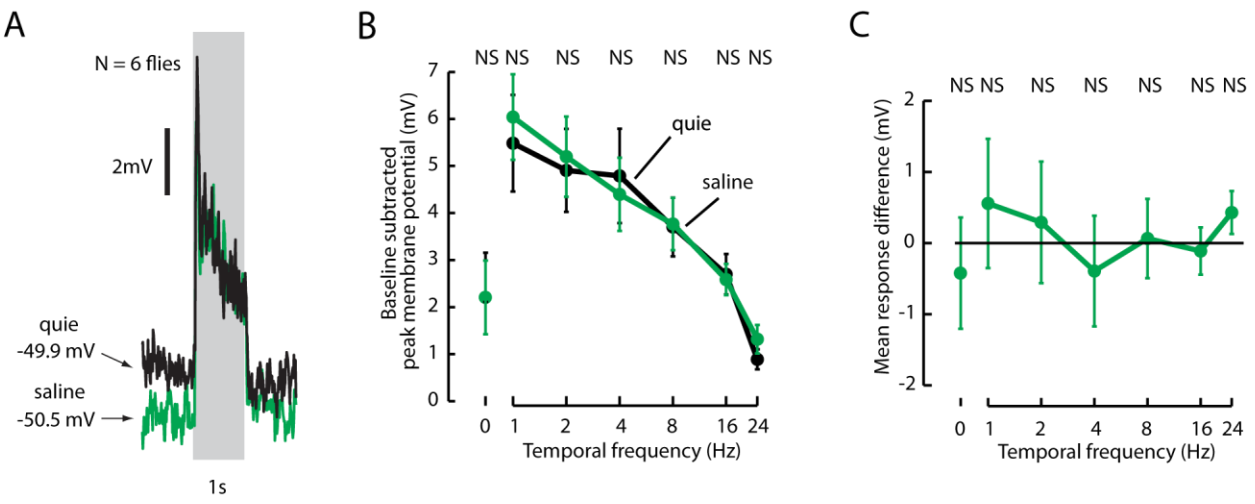

Figure S1, Related to Figure 2. Saline Control for Octopamine Pharmacology

(A) Average visual response to 8 Hz downward motion during saline application (green trace) and corresponding quiescent responses ('quie', black traces). The grey shaded region indicates when the visual stimulus was in motion. The average baseline membrane potential during the 1 s period immediately before motion onset is shown for quiescence and saline.

(B) Temporal frequency tuning curve for downward motion responses during quiescence and saline application. Abscissa is plotted on a log scale.

(C) Difference between motion responses during quiescence and saline application. Abscissa is plotted on a log scale. In B and C, NS indicates speeds at which the difference between saline and quiescent responses (computed for each fly) was not significantly greater than zero (paired Student's t-test, alpha = 0.05).

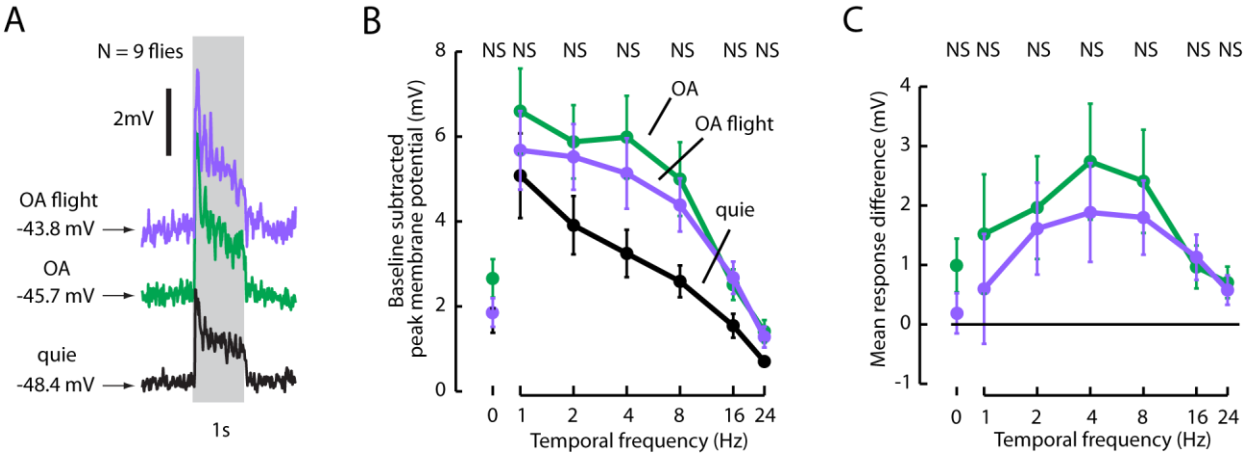

Figure S2, Related to Figure 2. Effect of Flight during Octopamine Application

(A) Average visual response to 8 Hz downward motion during quiescence ('quie', black traces), octopamine application (OA; green trace) and flight during octopamine application (OA flight; purple trace). The grey shaded region indicates when the visual stimulus was in motion. The average baseline membrane potential during the 1 s immediately before motion onset is shown for quiescence, OA and OA flight.

(B) Temporal frequency tuning curve for downward motion responses during quiescence, octopamine application, and flight during octopamine application. Abscissa is plotted on a log scale.

(C) Difference between motion responses during octopamine application and quiescence, and flight during octopamine application and quiescence. Abscissa is plotted on a log scale. In B and C, NS indicates speeds at which the difference between OA flight responses and OA responses (computed for each fly) was not significantly greater than zero (paired Student's t-test, alpha = 0.05).

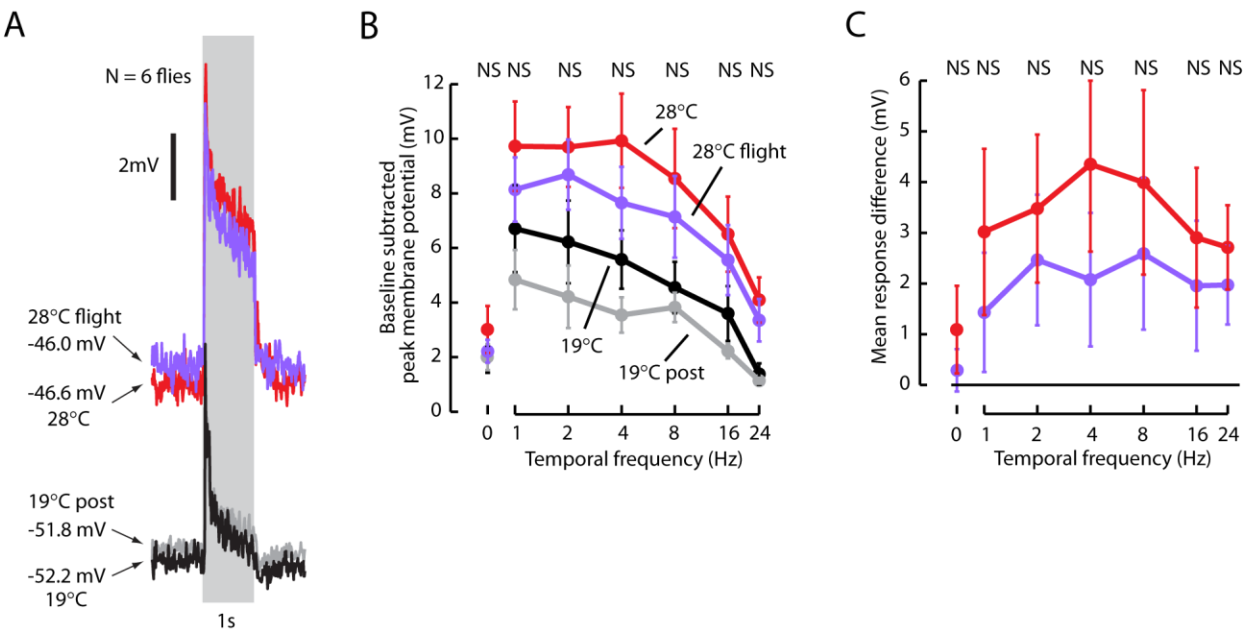

Figure S3, Related to Figure 4. Effect of Flight during Activation of Octopamine Neurons

(A) Average visual response to 8 Hz downward motion before (19°C, black trace), during (28°C, red trace), during while flying (28°C flight, purple trace), and after (19°C post, grey trace) dTrpA1 channels were activated in octopamine cells (*Tdc2-Gal4*, *UAS-dTrpA1*). Shaded light grey region indicates when the visual stimulus was in motion. Average baseline membrane potential during the 1 s immediately before motion onset is shown for each of these four conditions.

(B) Temporal frequency tuning curve for downward motion responses before, during, during while flying, and after dTrpA1 activation.

(C) Average response difference between during (28°C) and before (19°C) dTrpA1 activation, and between during while flying (28°C flight) and before (19°C) dTrpA1 activation. In B and C, NS indicates speeds at which the difference between 28°C flight responses and 28°C responses (computed for each fly) was not significantly greater than zero (paired Student's t-test, alpha = 0.05).

SUPPLEMENTAL EXPERIMENTAL PROCEDURES

Animals

We used 1-3 day old female *Drosophila melanogaster* raised on standard cornmeal medium at 25°C with a 14:10 light/dark schedule. To encourage long flight bouts, we removed the pro- and meso-thoracic legs.

Whole Cell Patch Clamp Recordings

We used electrodes with resistance of 4.8-7.4 MΩ. Our intracellular, external, and collagenase solutions were identical to those used in Maimon, et al. [6]. We added 20μM Alexa 568 (Invitrogen #A-10437) and 13mM biocytin (Invitrogen #B1093) to the intracellular solution for cell visualization. For 13 cells, we omitted biocytin and observed no obvious effect in the physiological responses. The average resting potential of cells after compensation for an experimentally-measured junction potential (-13mV) was -46.4mV. We injected 20-30pA constant hyperpolarizing current into the cells prior to presentation of visual stimuli to aid with dye fills, which decreased the membrane potential by an average of 3.6mV (to -50.0 mV). The access resistance (R_{acc}) for all recordings was 31.8 +/- 6.8 MΩ S.D., which is in the typical range for *Drosophila* whole-cell patch clamp recordings [43]. Any cells with R_{acc} greater than 50MΩ were excluded from our analysis.

We controlled the temperature of the bath with a bipolar temperature controller and an in-line heater/cooler (CL-100 and SC-20, Warner Instruments). For all experiments with the exception of dTrpA1-activation and parental controls, we raised the bath temperature to 30°C during the initial desheathing step, and then lowered the bath to temperature 19°C for the remainder of the experiment. We performed the desheathing without any applied heat in all dTrpA1 activation and parental control experiments to avoid contaminating results with pre-exposure to heat. For these dTrpA1 activation experiments, we held the external saline at 19°C, increased it to 28°C over a time course of approximately 120 seconds, and then lowered it back to 19°C.

Pharmacology

We dissolved octopamine (DL-Octopamine hydrochloride, Fluka) in extracellular saline at a concentration of 100μM on the day of each experiment. For comparison, this concentration of octopamine, the lowest level at which VS cell responses were noticeably and reliably affected, lies at or near concentrations used in previous studies in locusts [45, 46], crustaceans [47], and crickets [48]. We modified the holder from Maimon, et al. [6] to more rapidly apply octopamine by aiming the perfusion input directly towards the exposed neuropil. The cells never fully recovered to pre-octopamine levels of activity during a washout of octopamine, so we do not present these responses.

Immunohistochemistry

We dissected brains in 4% paraformaldehyde in PBS and fixed for a total of 30 min. We then incubated them overnight at 4°C in a primary antibody solution containing 5% normal goat serum in PBS-Tx, mouse anti-nc82 (1:10, DSHB) and rabbit anti-GFP (1:1000, Invitrogen). Brains were then incubated overnight at 4°C in a secondary antibody solution containing 5% normal goat serum in PBS-Tx, goat anti-mouse Alexa Fluor 633 (1:250, Invitrogen) and goat anti-rabbit Alexa Fluor 488 (1:250, Invitrogen). We then mounted the brains in Vectashield and imaged them on a Leica SP5 II confocal microscope under 40x magnification and scanned at 1μm section intervals. We adjusted intensity and contrast for single channels for the entire image using ImageJ 1.45s.

Calcium Imaging

We imaged the brain using the Prairie Ultima IV two-photon excitation microscope controlled by Prairie View Acquisition software (Prairie Technologies). We used a mode locked Ti:Sapphire laser (Chameleon Ultra; Coherent) tuned to 930 nm as an excitation light source and adjusted the laser power to be 20 mW at the rear aperture of the objective lens (Nikon NIR Ap, 40x water-immersion lens, 0.8 NA). We collected fluorescence using a multi-alkali photomultiplier tube (Hamamatsu) after bandpass filtering it with an HQ525/70m-2p emission filter (Chroma Technologies). We acquired

images in a frame scan mode (152x150 pixels, 0.125 s/frame) to record activity of octopamine neurons. For each trial, we acquired images for 30 s, starting from 10 s before the flight onset. For each fly, we acquired a z-stack image (z step = 1 μm) covering the entire dendritic branch of the octopamine neurons near the esophagus foramen to confirm the location of each recording within the brain.

Data Analysis and Statistics

For whole cell patch clamp recordings, we acquired data at 10 kHz using Axoscope software. All data analyses were done using Matlab R2010b. We calculated peak visual responses by first down-sampling the data to 1 kHz. We then calculated a moving average of the membrane potential over a window of 10 points (10 ms) and selected the peak during the first cycle of stimulus motion.

For two-photon imaging experiments, we applied a brief puff of air to the head of the fly to initiate flight, as in the electrophysiology experiments. If a fly was still flying after the end of two-photon image acquisition (approximately 20 s after the onset of flight), we terminated the flight by manually delivering a second puff of air. We waited 4 min between initiations of flight in the same animal. Only flies that flew for at least five bouts lasting 12 s or more were included in the analysis. Throughout the experiment, we illuminated the fly from behind with a high-intensity infrared diode (880nm; Golden Dragon; Osram) and used a Basler A602f camera with a fixed-focus lens (Infinistix 90, 94 mm working distance, 1.0x magnification) to record the behavior of the fly from below at 100 frames/s. We used FView [49], an open source program written in Python, to record images of flies simultaneously with a signal that indicates the timing of two-photon image acquisition. We analyzed images using custom software written in Matlab 2011b. We first smoothed the acquired images with a Gaussian filter (3 x 3 pixel, σ= 0.5) and corrected for small movements of the brain in the x-y direction during the image acquisition using a previously published algorithm [50]. We then averaged the pixel intensity in the ROI to estimate the fluorescence from this region. For each trial, we reviewed the images of flight behavior and determined the flight onset time by finding the first frame after the application of air puff where a fly moves its wing forward. We

then used the simultaneously recorded signal that indicates the timing of two-photon image acquisition to find the frame in the calcium imaging that corresponds to flight onset time. We used average fluorescence during the five s period before the onset of the flight as baseline fluorescence (F_0) and used this value to calculate the $\Delta F/F$ signal (defined as $(F-F_0)/F_0$). We calculated mean $\Delta F/F$ signal for each fly using 5 to 6 trials.